Models of TCP in High-BDP Environments and Their Experimental Validation

Gayane Vardoyan
University of Massachusetts Amherst
Email: gvardoyan@cs.umass.edu

Nageswara S. V. Rao
Oak Ridge National Laboratory
Email: raons@ornl.gov

Don Towsley
University of Massachusetts Amherst
Email: towsley@cs.umass.edu

***Abstract*—In recent years, there has been a steady growth in network bandwidths. This is especially true in scientific and big data environments, where high bandwidth-delay products (BDPs) are common. It is well-understood that legacy TCP (*e.g.* TCP Reno) is not appropriate for such environments, and several TCP variants were developed to address this shortcoming. These variants, including CUBIC, STCP, and H-TCP, have been studied in some empirical contexts, and some analytical models exist for CUBIC and STCP. However, since these studies were conducted, BDPs further increased, and new bulk data transfer methods have emerged that utilize parallel TCP streams. In view of these new developments, it is imperative to revisit the question: 'Which congestion control algorithms are best adapted to current networking environments?' In order to answer this question, (i) we create a general theoretical framework within which to develop mathematical models of TCP variants that account for finite buffer sizes, maximum window constraints, and parallel TCP streams; (ii) we validate the models using measurements collected over a high-bandwidth testbed and achieve low prediction errors; (iii) we find that CUBIC and H-TCP outperform STCP, especially when multiple streams are used.**

I. Introduction

The congestion collapse in the ARPANET during the late 1980s prompted the adoption of what is now referred to as legacy Transmission Control Protocol (TCP). Later, the advent of high-BDP networks stimulated the development of several TCP variants to overcome the inefficiencies of legacy TCP. These include HSTCP (HighSpeed TCP) [1], FAST (FAST AQM Scalable TCP) [2], BIC (Binary Increase Congestion control) TCP [3], STCP (Scalable TCP) [4], CUBIC TCP [5], and H-TCP (Hamilton TCP) [6]. To an extent, all of these Congestion Avoidance (CA) algorithms are successful in improving bandwidth utilization, although some exhibit better fairness, friendliness, and convergence properties than others. Several empirical studies of these algorithms exist ([7], [8], [9], [10], [11], among others), and although CUBIC is currently the default in Linux kernels, as of yet, there is no definitive consensus on which CA algorithm is best.

Adding to this uncertainty, many other studies rely either on simulations or networks with relatively low bandwidths compared to current High-Speed Network (HSN) environments. Today, 10 Gbps Wide Area Network (WAN) links are not uncommon between large-scale datacenters and computing facilities. An example is the Extreme Science and Engineering Discovery Environment (XSEDE) [12], a collection of supercomputing resources spanning several universities, national labs, and other research institutions, all interconnected by 10 Gbps (and sometimes faster) links. XSEDE offers tools like Globus GridFTP [13] and *sftp* for data transfers (note that FTP relies on TCP for reliable data movement), and such bulk data transfer mechanisms are becoming increasingly popular in HSNs.

Since BDPs have grown significantly and new bulk data transfer protocols that use parallel TCP streams have been introduced, it is important to reevaluate TCP both analytically and empirically. In this paper, we present a framework within which we derive analytical models for TCP variants. Unlike prior work, where models are studied in isolation for each TCP variant, our framework is not variant-specific and can be used to model a range of loss-based TCP variants. We use measurements on an experimental testbed to motivate and validate these models.

In some environments, researchers share WAN links for data transfers. The drawback is that TCP streams belonging to different users may compete for bandwidth and other resources. An alternate method of transferring data is through the use of virtual circuits (VCs) dedicated to a single user or application. One example is the On-Demand Secure Circuits and Advance Reservation System (OSCARS) [14], which allows users to reserve high-bandwidth VCs for guaranteed performance. According to the Energy Sciences Network, more than 50 research networks deploy OSCARS, including the US LHC Network; and OSCARS VCs carry half of the Department of Energy's (DOE) science traffic. The increasing popularity of VC-based data transfer options serves as excellent motivation to study TCP behavior in a controlled setting. Moreover, it provides an incentive to examine scenarios with only a fixed, rather than a dynamically changing, number of TCP connections.

Most protocols that strive to achieve efficient bulk data transfers do so by providing features that allow users to tune them as they see fit. For example, GridFTP supports both parallelism and concurrency (parallel streams use one socket and concurrent streams use separate sockets; henceforth, we use these terms interchangeably). It has become clear that the reason for the emergence of tools like GridFTP is the fact that TCP is not able to keep up with the demands of today's high-BDP networks. In this paper, we develop a framework that enables us to study the performance of protocols like GridFTP in dedicated high-BDP networks. To do so, we concentrate on a possible underlying root cause of poor bandwidth utilization: the congestion control (CC) algorithms used by all TCP-based data transfer tools.

We take two approaches in an attempt to understand the dynamics of TCP in modern environments: (i) first-principled modelling and (ii) measurement-based. We create robust, detailed analytical models of variants of the protocol. At the same time, we evaluate these variants on a dedicated network link, in a controlled setting that allows us to emulate diverse experimental configurations while removing any interference (*e.g.* I/O, background traffic) that could obscure TCP's intended behavior. We collect detailed measurements of memory-to-memory transfers on two different testbed configurations using *iperf* and *tcpprobe*, for three different TCP variants.

The main contributions of this work are:

- A general and comprehensive framework for modelling a diverse set of congestion control algorithms. The framework encompasses not only congestion avoidance, but also the slow-start mechanism. The latter takes into consideration the heuristic guidelines imposed by Hybrid slow-start (HyStart) [15], which is the implementation of slow-start used in current Linux kernels.
- A validation of these models using an extensive set of measurements.
- Last, we observe from our measurements that (i) CUBIC and H-TCP are comparable in terms of average throughput, while they both outperform STCP, and (ii) TCP performance benefits from the presence of a well-designed physical layer (*e.g.* SONET).

We use only first principles to model the performance of each TCP variant in terms of its average throughput as a function of round trip time (RTT). The models also accept link capacity, buffer size, transfer size, number of parallel streams, and maximum congestion window (*cwnd*) size as parameters. Using measurements, we validate the models and compare the performance of the TCP variants. *To our knowledge, this work constitutes the first careful measurement-based modelling study of TCP congestion control algorithms in a high-BDP/HSN setting.*

The remainder of the paper is organized as follows. We describe the three variants and related work in Section II. In Section III, we describe the testbed, measurement collection, and first-hand observations from the collected data. In Section IV, we delve into the analytical framework for slow-start, congestion avoidance, and each of the variants separately, presenting closed-form expressions for sending rate where possible. In Section V, we present and validate our results. Finally, we conclude the paper in Section VI.

II. Background

A. TCP Variants

We study CUBIC because it is the most commonly used variant in current HSN networks and the default CA algorithm in the Linux kernel. Unlike most TCP variants, CUBIC is not an acknowledgement (ACK)-based algorithm. Instead, CUBIC's *cwnd* is a cubic function of time since the last congestion event such that the inflection point is the maximum window size immediately before the most recent loss occurred.

We also study STCP because it was developed within the optimization-based framework proposed in [16]. STCP is a multiplicative increase, multiplicative decrease (MIMD) [1] algorithm with the following response functions:

$$\mathit{cwnd} \leftarrow \mathit{cwnd} + a$$

for every ACK received, where the increase factor a is usually set to 0.01. Upon loss detection,

$$\mathit{cwnd} \leftarrow b * \mathit{cwnd}$$

Usually, $b = 0.875$ for STCP.

Finally, we study H-TCP because of its favorable fairness and convergence properties [8]. H-TCP is an ACK-based generalized additive increase multiplicative decrease (AIMD) algorithm whose additive increase factor a is a function of the time t since the last congestion event. Specifically, a is defined as:

$$a \leftarrow 2(1-b)a(t)$$

where $a(t)$ is

$$a(t) = \begin{cases} 1 & t \leq \Delta^L \quad \text{(1a)} \\ 1 + 10(t - \Delta^L) + \left(\dfrac{t-\Delta^L}{2}\right)^2 & t > \Delta^L \quad \text{(1b)} \end{cases}$$

Δ^L is usually set to one second so that for small congestion epochs, H-TCP behaves like standard TCP. H-TCP's decrease factor b is defined as

$$b \leftarrow \frac{RTT_{min}}{RTT_{max}}, \; b \in [0.5, 0.8]$$

where RTT_{min} and RTT_{max} are the minimum and maximum measured RTTs of a flow. Upon loss detection, *cwnd* is updated as follows:

$$\mathit{cwnd} \leftarrow b * \mathit{cwnd}$$

B. Related Work

There exist a number of analytical studies for modelling TCP. Kelly proposed an optimization-based framework for studying and designing CA algorithms in [16], where STCP was an output. In [17], Srikant presented a simple analysis of Jacobson's TCP CC algorithm. The derivation sets the maximum window constraint to the sum of the BDP and the size of the buffer. Our analysis is more refined in that it takes into consideration two different maximum window constraints, as discussed in Section IV. A model for slow-start is also presented in [17]. We extend this model by considering the latest version of slow-start currently in use by Linux kernels.

In [18], Misra *et al.* model TCP throughput using stochastic differential equations. El Khoury *et al.* [19] present a model for STCP that includes buffer size as a parameter, but only in the

[1]Note that although the per-ACK update rule for STCP is additive, this CA algorithm is MIMD at the RTT level.

case of a very small buffer. In addition, they rely only on *ns-2* simulations for validation. Bao *et al.* propose Markov chain models for average CUBIC throughput, but for a wireless environment [20]. Moreover, they do not directly account for buffer constraints. Leith *et al.* present empirical evidence that H-TCP fares well in bandwidth utilization compared to other TCP variants [21], but the protocol's CC dynamics have not been analyzed in-depth.

There are some empirical studies that explore the behavior of TCP with multiple concurrent flows. Morris looks at a number of performance metrics using simulations and real packet traces, but does not explore different TCP variants [22]. Yu *et al.* compare the performance of three open-source big data transfer protocols in [23] using memory-to-memory transfers on a 10 Gbps international HSN. Bateman *et al.* compare different TCP variants for fairness at high speeds using *ns-2* and Linux [24]. As far as we know, no previous work attempts to model TCP with multiple flows using first principles.

III. Measurements

A. Emulation Testbed

Our testbed consists of two types of Linux hosts: 32-core and 48-core HP ProLiant servers, each with Broadcom 10 GigE NICs, running Linux 2.6 kernel (CentOS release 6.6). It also consists of ANUE OC192 and IXIA 10 GigE hardware connection emulators, and a 10 Gbps Force10 E300 WAN-LAN switch. Two separate configurations are utilized for 10 GigE and SONET measurements. These hardware connection emulators transport the physical packets between hosts, delaying them during transit by an amount specified at configuration. This process closely matches the effects of physical connections, particularly, the TCP dynamics of hosts connected to them, which in turn determine the throughput rates achieved. They more closely capture the real-time TCP dynamics compared to packet-level simulators (such as *ns-3* and *OPnet*) that are typically driven by discrete "packet delivery events".

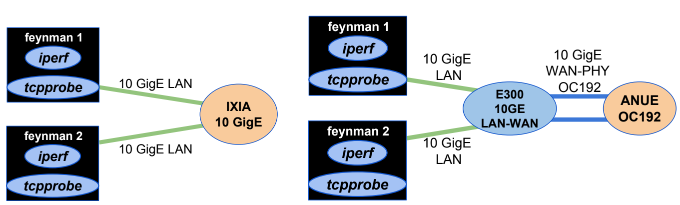

(a) 10 GigE (b) OC192

Fig. 1: Two testbed configurations for dedicated 10 Gbps connections.

We consider two configurations that use OC192 and 10 GigE physical layer modalities. In the first configuration, 10 GigE NICs of host systems are directly connected to two IXIA emulator ports as shown in Figure 1(a). Long range 1250 nm optical transceivers are used on host NICs to communicate directly with the emulator. The SONET configuration shown in Figure 1(b) is more complicated compared to the 10 GigE case, since hosts are equipped with 10 GigE NICs and do not support SONET. In this case, the 10 GigE NICs are connected to a Force10 E300 switch using multi-mode 850 nm optical transceivers in LAN-PHY mode. The E300 switch converts between 10 GigE LAN-PHY and WAN-PHY frames that are inter-operable with OC192 frames; the latter are sent through its WAN ports, which are directly connected to OC192 ANUE emulator ports as shown in Figure 1(b). We note that the peak capacity of an OC192 connection is 9.6 Gbps. We utilize these emulators to collect TCP measurements for a suite of dedicated connections where we set the RTT to 11.8, 22.6. 45.6, 91.6, 183 and 366 ms. RTTs in the mid-range represent US cross-country connections, for example, ones between DOE sites provisioned using the OSCARS system. Higher RTTs represent transcontinental connections.

B. Measurement Collection

We collect TCP measurements for three TCP CC modules: CUBIC, STCP, and H-TCP (all available as loadable modules under the Linux 2.6 distribution). Two types of measurements are collected in each case.

(a) *Throughput measurements* for memory-to-memory transfers are collected using *iperf*. In addition, intermediate throughput values from *iperf* at one-second intervals are collected for a more detailed analysis.
(b) *Kernel traces:* Certain TCP variables including *cwnd*, are collected using the *tcpprobe* kernel module to support a more detailed analysis and parameter estimates for analytical models. In this case, *tcpprobe* is configured to collect *tcp_info* variables each time a TCP segment is processed.

The *iperf* and *tcpprobe* traces are collected concurrently to facilitate the correlation of TCP parameters with throughput. Each test regimen is executed using a *bash* script that coordinates the setup of parameters for emulators, invocation of *iperf* and *tcpprobe* codes and collection of their outputs.

C. Empirical Observations

It is interesting to note the differences in measurements produced by the SONET and 10 GigE links. In general, we observe that the data obtained from SONET is well-behaved and more deterministic than that collected from 10 GigE. Figure 2 illustrates the stark contrast in TCP behavior between these two testbeds. The evolution of *cwnd* over time exhibits a consistent sawtooth pattern for SONET, whereas the 10 GigE transfer experiences non-uniformly-spaced losses and seemingly flat regions for smaller RTTs. The data shown is for STCP, for RTTs of 91.6 ms and 183 ms, although the results are consistent across different variants and other RTT values. These differences are important: they mean that for accurate predictions, the models must account for both the frequency of losses and the shapes of the *cwnd* curves. Section IV goes into specifics on how this can be accomplished.

Figures 2(c) and 2(d) reveal another difference between these two modalities: 10 GigE has more aggregate buffer space than SONET. Visually, buffering occurs when *cwnd* grows as

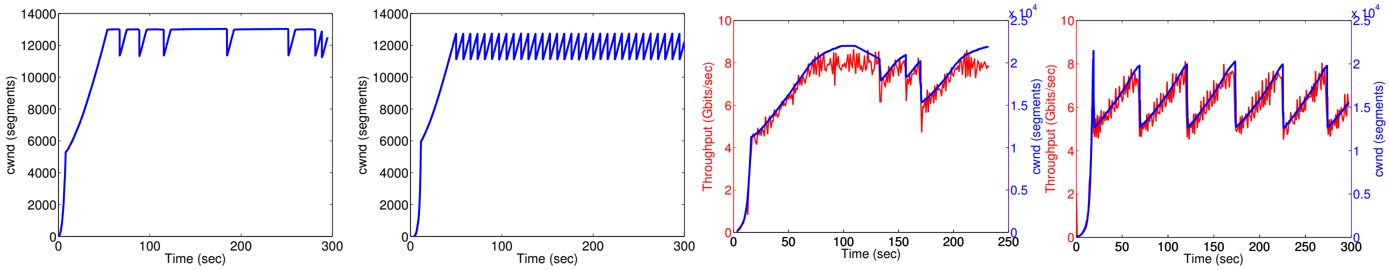

(a) RTT=91.6 ms, 10 GigE (b) RTT=91.6 ms, SONET (c) RTT=183 ms, 10 GigE (d) RTT=183 ms, SONET

Fig. 2: Comparisons between 10 GigE and SONET measurements. TCP variant: STCP. (a) and (b) show *tcpprobe*. (c) and (d) show both *iperf* and *tcpprobe*.

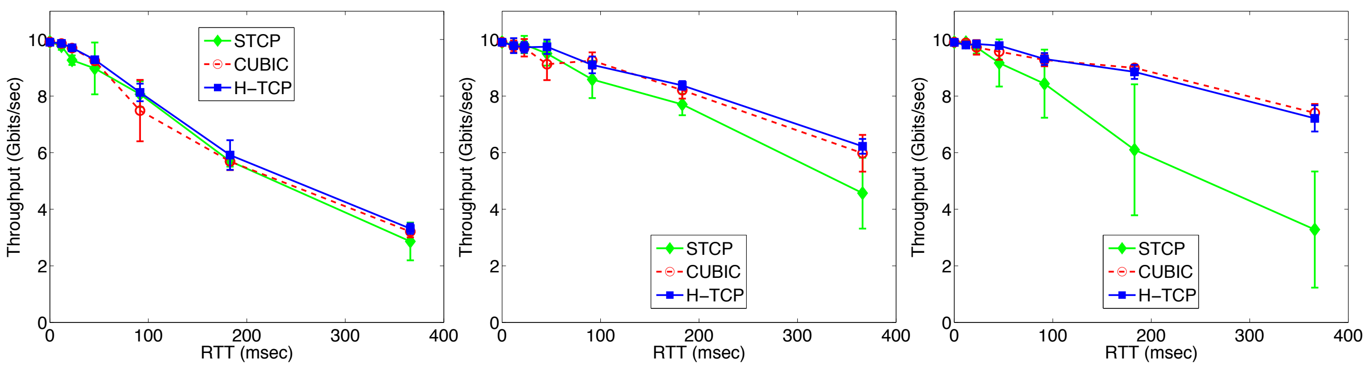

(a) three streams (b) seven streams (c) ten streams

Fig. 3: Comparison of STCP, CUBIC, and H-TCP average throughputs on the 10 GigE testbed.

throughput remains relatively constant. The size of the buffer corresponds to the white space between the two curves, and since it is more prevalent in 10 GigE data, we know that this configuration has the larger buffer size. Figure 3 presents a comparison of the three variants in terms of their average throughput. The dataset was collected over the 10 GigE link. Each memory-to-memory flow was active until it transferred 10 GB of data. It is evident that for a small number of streams, the three variants perform almost equally well. However, as the number of flows grows, the differences in performance become more notable: CUBIC and H-TCP significantly outperform STCP with ten parallel flows.

IV. Analysis

We first present a model for slow-start and discuss how it can accommodate an important component of HyStart. Then, we present single-stream analytical models for two different types of loss-based congestion avoidance mechanisms: (i) those that are ACK-based and (ii) those that grow *cwnd* as a function of time since last loss (referred to as TSL-based variants). STCP and H-TCP are ACK-based, while BIC and CUBIC are examples of TSL-based algorithms. Finally, we demonstrate how single-stream models can easily be extended to incorporate multiple parallel TCP streams.

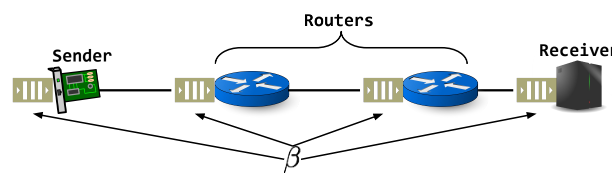

Fig. 4: Buffer size β on a network. This includes buffers at sender and receiver network interfaces, and routers.

Table I contains definitions of variables used in this section. We assume that we know the link capacity C, aggregate buffer size β, round-trip-time τ, size of the transfer F, and increase or decrease parameters. The minimum RTT, τ, is the delay measured before the buffer of size β begins to fill up. This can be measured by running a simple *ping* command between the source and receiver. β represents the aggregate size of all buffers present on the link (*e.g.* on routers and NICs). An illustration is shown in Figure 4. W_{max} is a constraint on *cwnd* typically imposed by the receiver (receive-window).

A. Slow-Start

In traditional slow-start, *cwnd* approximately doubles every round trip time of length τ in which loss is not detected:

$$w(t) = 2^{t/\tau}$$

TABLE I: Variable definitions used in analysis.

Variable	Definition	Unit
C	link capacity	bits/sec
τ	minimum round trip time	sec
$w(t)$	*cwnd* as function of time	bits
W_{max}	maximum window constraint	bits
W_m	size of *cwnd* immediately before loss	bits
β	aggregate buffer size	bits
S	sending rate	bits/sec
Θ	throughput	bits/sec
$ssthresh$	slow-start threshold	bits
a	additive or multiplicative increase factor	N/A
b	multiplicative decrease factor	N/A
F	file size	bits
k	number of CA epochs for a transfer	N/A
n	number of parallel TCP flows	N/A

Slow-start ends at time T_s, when $w(t)$ reaches $ssthresh$ and CA begins.

$$T_s = \tau \log_2(ssthresh) \tag{2}$$

The amount of data transferred during time T_s is N_s:

$$N_s = \frac{1}{\tau}\int_0^{T_s} 2^{t/\tau} dt = \frac{2^{t/\tau}}{\ln(2)}\Big|_0^{T_s} = \frac{ssthresh - 1}{\ln(2)} \tag{3}$$

These expressions are accurate when $C\tau$ (the BDP) is greater than or equal to $ssthresh$. In HSN environments, this is a reasonable assumption that is validated by the measurements (see Figure 2 for examples).

At the time of writing, HyStart is the default slow-start algorithm used in Linux. This algorithm uses the same *cwnd* growth function as traditional slow-start. According to [15], HyStart sets an upper bound on *cwnd* equal to $C_a\tau/2 + \beta_a$, where C_a is the available bandwidth and β_a is the available buffer space. There is also a lower bound on *cwnd* equal to $(C_a\tau)/2$. In real scenarios (especially where packet loss is highly prevalent), it is likely that the value of $ssthresh$ will change several times during the lifetime of a TCP flow. However, for highly-reliable, dedicated connections, such as ones encountered in HSN settings, it is safe to assume that a flow will enter slow-start only once (in the beginning of a transfer), and afterward will likely remain in CA state. This assumption is further validated by our *tcpprobe* measurements. In this case, only one estimate of $ssthresh$ is required. At the beginning of a connection, most of the link capacity and buffer space are unused. Hence, we let $ssthresh = C\tau/2+\beta$, which proves to work quite well in practice; in fact, we find it much better to model $ssthresh$ as a function of τ, rather than leaving it as a constant.

B. Congestion Avoidance

For all TCP variants, CA consists of two phases. Figure 5 illustrates them using generic *cwnd* curves (not specific to any TCP variant). The goal is to derive expressions for N_a, the amount of data transferred during one such CA epoch, and T_a, the duration of one CA epoch. The number of CA epochs for a given transfer is approximately

$$k = \frac{F - N_s}{N_a}.$$

The sending rate S can be approximated as

$$S = \frac{N_s + kN_a}{T_s + kT_a}.$$

Then, throughput Θ can be estimated as

$$\Theta = S(1-p)$$

where p is the packet loss probability for a TCP flow. For small values of p,

$$\Theta \approx S$$

Next, we discuss how to obtain N_a and T_a for various cases.

Case 1: $W_{max} \leq C\tau$. In Phase I, *cwnd* grows until either the link capacity or W_{max} is reached (if $W_{max} \leq C\tau$). In the latter case, *cwnd* remains flat until the transfer ends, buffer overflow never occurs, and there is no second phase. The amount of data transferred in this case is $N_a = F - N_s$ (file size minus the amount of data transferred in slow-start), and since the sending rate is capped at W_{max}/τ, it takes $T_a = N_a\tau/W_{max}$ time until the transfer ends.

Case 2: $W_{max} > C\tau$. In this case, each congestion epoch will have two phases.

Phase I: The methodology for obtaining N_0 and T_0 for Phase I is the same for ACK-based and TSL-based variants. Given a congestion window function $w(t)$, we know that:

$$w(T_0) = C\tau.$$

Using this relation, we can solve for T_0: either directly (if $C\tau < W_{max} < W_m$ as in Figure 5b) or in terms of W_m (if $W_{max} \geq W_m$ as in Figure 5a). In order to distinguish between 5b and 5a, we must first solve for W_m (discussed below). The amount of data transferred in Phase I is:

$$N_0 = \frac{1}{\tau}\int_0^{T_0} w(t)dt.$$

Phase II: In Phase II, the sending rate is capped at C, and the buffer begins to fill up. We first solve for W_m with the hypothesis that 5a is the correct representation of our congestion epoch. Once a value for W_m is obtained, this hypothesis can be rejected or accepted by comparing W_m with W_{max}. However, how we solve for W_m depends on the type of CA mechanism.

1) ACK-Based CA: The following ordinary differential equation (ODE) describes the behavior for ACK-based TCP variants:

$$\frac{\partial w}{\partial t} = \frac{\partial w}{\partial A}\frac{\partial A}{\partial t} \tag{4}$$

where A represents an acknowledgement. Since the sending rate is C, this is also the rate at which ACKs are being received:

$$\frac{\partial A}{\partial t} = C.$$

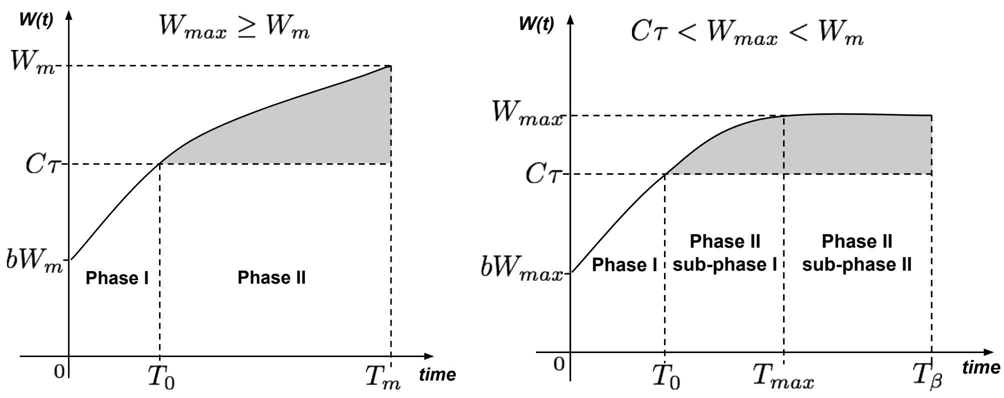

(a) (b)

Fig. 5: Example *cwnd* curves for one congestion avoidance epoch, with (a) and without (b) a W_{max} constraint. Shaded areas are the size of the buffer.

For every ACK, *cwnd* increases by a, so

$$\frac{\partial w}{\partial A} = a.$$

Hence,

$$\frac{\partial w}{\partial t} = Ca. \tag{5}$$

The initial condition for this ODE is $w(0) = C\tau$. The ODE can now be solved to obtain a window function for Phase II, $w_2(t)$.

2) TSL-Based CA: In a TSL-Based variant, *cwnd* grows identically in Phase II as it does in Phase I. Hence, $w_2(t) = w(t)$.

Now that we have $w_2(t)$, we make the following useful observations:

$$w_2(T_m) = W_m, \tag{6}$$

$$N_m = \frac{1}{\tau}\int_0^{T_m} w_2(t)dt, \tag{7}$$

$$N_m - CT_m - \beta = 0. \tag{8}$$

Using (6), we can solve for the duration of Phase II, T_m, in terms of W_m. The amount of data transferred in Phase II, N_m, is given by (7), also in terms of W_m. Finally, we obtain a value for W_m by finding the roots of (8) and selecting the appropriate root (subject to the constraints that $W_m \in \mathcal{R}$ and $W_m \geq C\tau$).

Subcase 1: $W_m \leq W_{max}$. In this case, we simply substitute the value of W_m into the expressions for T_m, N_m, T_0 and N_0. Then,

$$N_a = N_0 + N_m,$$
$$T_a = T_0 + T_m.$$

Subcase 2: $W_m > W_{max}$. In this case, 5b correctly depicts the shape of the congestion epoch. Since W_{max} is known, we can solve for T_{max}, the duration of sub-phase I of Phase II, directly:

$$w_2(T_{max}) = W_{max}.$$

The amount of data transferred during this sub-phase is

$$N_{max} = \frac{1}{\tau}\int_0^{T_{max}} w_2(t)dt.$$

The only unknown left is T_β, the duration of sub-phase II, and N_β, the amount of data transferred during that interval. However, we know that during sub-phase II, the sending rate is capped at W_{max}/τ, so

$$N_\beta = \frac{W_{max}}{\tau}T_\beta.$$

We can solve the following equation for T_β:

$$N_{max} + N_\beta - C(T_{max} + T_\beta) - \beta = 0.$$

Then,

$$N_a = N_0 + N_{max} + N_\beta,$$
$$T_a = T_0 + T_{max} + T_\beta.$$

C. Examples

We demonstrate the versatility of the generalized modelling framework described in previous sections through three examples: STCP and H-TCP (both ACK-based variants) and CUBIC (a TSL-based variant).

1) STCP: Since the additive increase factor for STCP is a constant, the solution to the ODE in (5) is simply

$$w_2(t) = C(at + \tau). \tag{9}$$

Using this equation, we obtain:

$$T_m = \frac{W_m - C\tau}{Ca},$$
$$N_m = \frac{W_m^2 - (C\tau)^2}{2Ca\tau},$$
$$W_m = C\tau + \sqrt{2Ca\tau\beta}.$$

If $W_m \leq W_{max}$, we have everything we need for Phase II. Otherwise, we use W_{max} instead of W_m in the expressions for T_m and N_m; this gives us T_{max} and N_{max}:

$$T_{max} = \frac{W_{max} - C\tau}{Ca},$$
$$N_{max} = \frac{W_{max}^2 - (C\tau)^2}{2Ca\tau}.$$

Further,

$$T_\beta = \frac{\beta\tau}{W_{max} - C\tau} - \frac{W_{max} - C\tau}{2Ca}.$$

This completes the analysis for Phase II. We now analyze Phase I by first constructing an ODE that describes *cwnd* growth before the BDP is reached:

$\frac{\partial w}{\partial A} = a$ as in Phase II, but since S is below C, $\frac{\partial A}{\partial t} = \frac{w}{\tau}$.

The final ODE and its solution are:

$$\frac{\partial w}{\partial t} = \frac{w}{\tau}a,$$
$$w(t) = ge^{at/\tau} \text{ where } g \text{ is a constant,}$$
$$w(0) = bW_m = g,$$
$$w(t) = bW_m e^{at/\tau}. \tag{10}$$

Next, we can solve for T_0 and N_0:

$$T_0 = \frac{\tau}{a}\ln\left(\frac{C\tau}{bW_s}\right),$$
$$N_0 = \frac{C\tau - bW_s}{a}$$

where

$$W_s = \min(W_m, W_{max}). \tag{11}$$

This completes the analysis for STCP.

2) CUBIC: Because CUBIC is not ACK-based, there is no need to derive two different window functions for its analysis: $w(t)$ grows as follows for both phases:

$$w(t) = c\left(t - \sqrt[3]{\frac{bW_s}{c}}\right)^3 + W_s \tag{12}$$

where W_s is defined in (11), t is the time since the last congestion event in unit of RTT, c is a scaling factor (usually equal to 0.4), and b is a multiplicative decrease factor usually equal to 0.2.

We present the closed-form solutions for the necessary variables. Since CUBIC is TSL-based, it helps to think of T_0 and T_m as points in time that delimit the phases, rather than durations of phases (let T_β remain as the duration of sub-phase II of Phase II).

$$T_m = \sqrt[3]{\frac{bW_m}{c}},$$
$$N_m = \frac{W_m}{\tau}\sqrt[3]{\frac{bW_m}{c}}\left(1 - \frac{b}{4}\right),$$
$$T_0 = \sqrt[3]{\frac{C\tau - W_m}{c}} + \sqrt[3]{\frac{bW_m}{c}}.$$

Above, N_m is the amount of data transferred in the interval $[0, T_m]$. Let N_1 be the amount of data transferred in the interval $[T_0, T_m]$.

$$N_1 = \frac{1}{\tau}\int_{T_0}^{T_m} w(t)dt = -\frac{1}{\tau}\sqrt[3]{\frac{C\tau - W_m}{c}}\left(\frac{C\tau + 3W_m}{4}\right),$$
$$N_1 - C(T_m - T_0) - \beta = 0.$$

The last equation above can be solved for W_m:

$$W_m = C\tau - \sqrt[4]{c\left(\frac{4\beta\tau}{3}\right)^3}.$$

Since we know that $W_m > C\tau$, we must take the negative root of the fourth-root term above. If W_m is indeed less than or equal to W_{max}, then the sending rate is

$$S = \frac{N_s + kN_m}{T_s + kT_m}.$$

Otherwise, we use W_{max} in the expressions for T_m and N_m above to obtain T_{max} and N_{max}, respectively. Also,

$$T_\beta = \frac{\beta - N_{max} - C\sqrt[3]{\frac{C\tau - W_{max}}{c}}}{\frac{W_{max}}{\tau} - C}.$$

Finally, S is

$$S = \frac{N_s + k\left(N_{max} + N_\beta\right)}{T_s + k(T_{max} + T_\beta)}.$$

3) H-TCP: We do not present closed-form solutions for H-TCP, since they are too complex; the majority of the computations for this variant were performed using `Matlab`. Since Δ^L is usually set to one second, for simplicity we use it in the derivations below. We present the non-trivial case, in which the transfer lasts for $T_s + 1$ seconds. For H-TCP, let T_0, T_m, T_{max}, and T_β be points in time, rather than phase durations. For the first second of CA, H-TCP uses the increase function shown in (1a). The *cwnd* function is then

$$w_1(t) = bW_m + \frac{2(1-b)t}{\tau}.$$

The amount of data transferred during this time is N_{Δ^L},

$$N_{\Delta^L} = \frac{1}{\tau}\int_0^{T_{\Delta^L}} w_1(t)dt$$

where

$$T_{\Delta^L} = \min\left(1s, \frac{\tau(C\tau - bW_m)}{2(1-b)}\right).$$

This constraint on T_{Δ^L} is required because it may take less than one second for $w_1(t)$ to reach $C\tau$.

After the first second of CA, if $w_1(1) < C\tau$, H-TCP's increase function changes as shown in (1b). The *cwnd* function changes to

$$w_2(t) = w_1(1) + \frac{2(1-b)t}{\tau}\left(1 + 10(t-1) + \left(\frac{t-1}{2}\right)^2\right)$$

until *cwnd* reaches $C\tau$ at time T_0. N_0, the amount of data transferred in the interval $[0, T_0]$, is:

$$N_0 = \begin{cases} N_{\Delta^L}, & \text{if } T_{\Delta^L} \le 1s, \\ N_{\Delta^L} + \frac{1}{\tau}\int_1^{T_0} w_2(t)dt, & \text{otherwise.} \end{cases}$$

T_0 can be isolated from the relation $w_2(T_0) = C\tau$. After T_0 seconds have passed, the *cwnd* function changes again because the transfer transitions into Phase II. This new function is described by the ODE in (5), which uses the increase function shown in (1a) or (1b) depending on the value of T_{Δ^L}:

$$\partial w = aC\partial t,$$
$$w_3(t) = 2(1-b)C\int a(t)dt,$$
$$w_3(T_0) = C\tau \text{ is the initial condition.}$$

H-TCP then uses $w_3(t)$ for the rest of the congestion epoch, which ends at time T_m. It is possible to solve for T_m in terms of W_m using the relation $w_3(T_m) = W_m$. The amount of data transferred during Phase II is N_m:

$$N_m = \frac{1}{\tau}\int_{T_0}^{T_m} w_3(t)dt.$$

It is now possible to solve for W_m using the following equation:

$$N_m - C(T_m - T_0) = \beta.$$

If $W_{max} \ge W_m$, then S is:

$$S = \frac{N_s + k(N_0 + N_m)}{T_s + kT_m}.$$

Otherwise, T_β must be determined using a similar technique used for STCP and S changed to:

$$S = \frac{N_s + k\left(N_0 + \frac{1}{\tau}\int_{T_0}^{T_{max}} w_3(t)dt + \frac{W_{max}}{\tau}(T_\beta - T_{max})\right)}{T_s + kT_\beta}$$

D. Parallel Flows

We now present a simple, yet effective modification to the single-stream modelling framework presented above to accommodate multiple flows. The main idea is to model n parallel flows as a single, more aggressive flow. The modifications are as follows:

1) For any single-flow TSL-based CA *cwnd* function $w(t)$, the multiple-flow *cwnd* function is $w(nt)$, where n is the number of flows. For any single-flow ACK-based CA *cwnd* function, the multiple-flow *cwnd* function is obtained by multiplying the increase factor (as in the case of STCP) or the increase function (as in the case of H-TCP) by n. The only exception to this rule are *cwnd* functions in Phase II of ACK-based CA variants, which must be left unchanged. For example, STCP's (10) becomes

$$w(t) = bW_m e^{ant/\tau}$$

while (9) remains the same. The reason for this is that once an ACK-based variant transitions into Phase II, ACKs continue to arrive at a constant rate, so that there is no added advantage of using multiple flows past the point where *cwnd* $> BDP$. TSL-based variants, on the other hand, continue to grow the aggregate *cwnd* at a rate approximately n times faster than with a single flow, for as long as congestion is not detected.

2) W_{max} gets scaled up by a factor of n. However, there must be a hard constraint, W_{maxH}, on the aggregate *cwnd*, imposed by memory and buffer limitations. Therefore,

$$W_{max} = \min(nW_{max}, W_{maxH}).$$

3) In slow-start, we keep the duration (T_s) the same as for single flows, but multiply N_s by n. In addition, instead of $ssthresh$, we use

$$thresh = \min(ssthresh, C\tau/n, W_{max}).$$

Interestingly, Crowcroft *et al.* have previously explored a related idea, but as a means of delegating some flows a higher fraction of the bandwidth on a network [25]. They propose a controller, MulTCP, that attempts to increase the throughput of a single flow by a factor of n by scaling the flow's additive increase parameter by the same amount . Simulations showed that MulTCP does indeed achieve a sending rate of approximately nS as long as n is not too large.

V. Model Performance

Figure 6 shows throughput predictions for one, five, and ten H-TCP streams (we also did this for two-four and six-nine streams, not shown here). Measurement data obtained from the 10 GigE testbed is also presented in the figure and serves as validation for the models. The predictions were obtained using models presented in Section IV. Figure 7 shows the result of using the multiple-stream models to predict the throughput of one, two, four, six, eight, and ten parallel STCP flows (we also did this for three, five, seven, and nine streams, not shown here). Figure 8 shows the same for CUBIC.

We use different β and W_{max} parameter values for prediction in each dataset (although β and W_{max} are kept constant within a dataset). Note the odd 'dip' in throughput in Figure 7a for RTTs 11.8ms and 22.6ms: this is believed to be an anomaly. Let average error be defined as follows:

$$E = \frac{100}{|RTTs|}\sum_{r\in RTTs}\frac{|M_r - P_r|}{M_r}$$

where M_r and P_r are the measured and predicted throughputs, respectively, for RTT $= r$. The mean errors (averaged across all RTTs and $n \in \{1, \ldots, 10\}$) for multiple-stream predictions are as follows: 5.2% for H-TCP, 9.3% for STCP, and 4.5% for CUBIC.

VI. Conclusion

In this work, we have derived a unifying scheme for analyzing single-stream and multiple-stream memory-to-memory TCP transfers. We performed a detailed analysis for a diverse set of TCP variants: STCP – a MIMD algorithm; CUBIC – a non-ACK-based algorithm; and H-TCP – an adaptive AIMD algorithm. The models that emerged from this analysis were

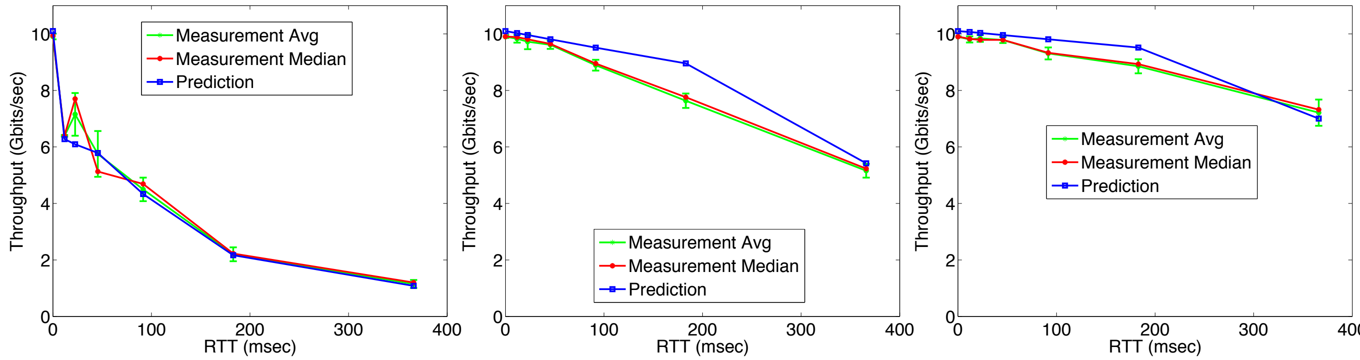

(a) one stream (b) five streams (c) ten streams

Fig. 6: Measurement averages and medians vs multiple-stream model predictions for H-TCP.

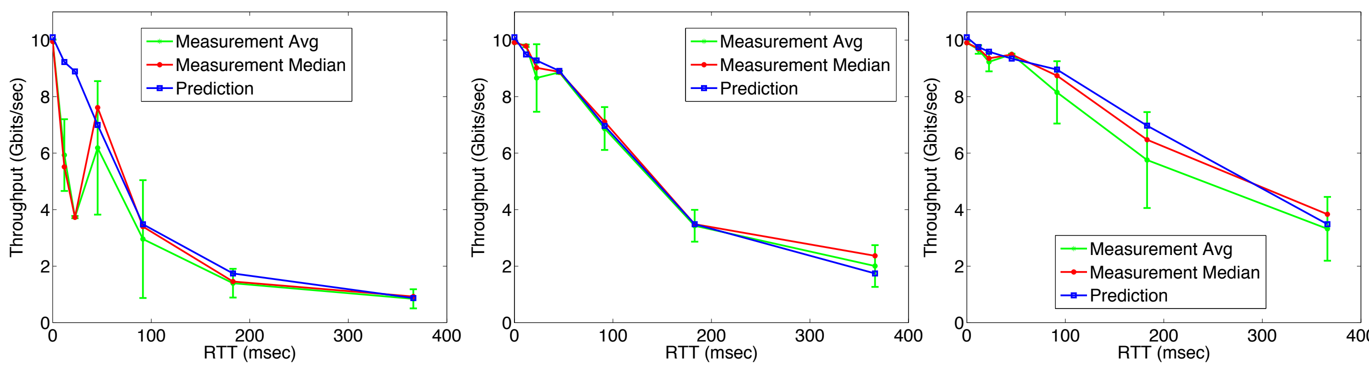

(a) one stream (b) two streams (c) four streams

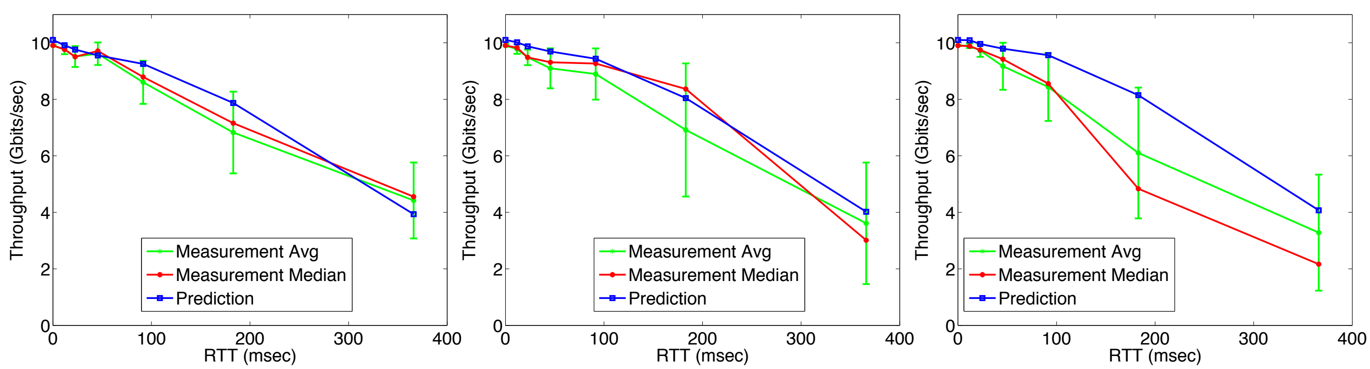

(d) six streams (e) eight streams (f) ten streams

Fig. 7: Measurement averages and medians vs multiple-stream model predictions for STCP.

validated using an extensive set of measurements. The results show that our models can be used to achieve accurate and reliable throughput predictions. The measurements independently show that CUBIC and H-TCP consistently outperform STCP, and the difference in performance becomes more pronounced as the number of parallel flows grows. In future work, we plan to expand the analysis to include (a) exogenous and time-variant loss, (b) I/O constraints, and (d) considerations of fairness and convergence.

VII. Acknowledgement

This work was supported in part by the US Department of Energy under Contract DE-AC02-06CH11357.

References

[1] S. Floyd, "HighSpeed TCP for large congestion windows," 2003.

[2] D. X. Wei, C. Jin, S. H. Low, and S. Hegde, "FAST TCP: motivation, architecture, algorithms, performance," *IEEE/ACM Transactions on Networking (ToN)*, vol. 14, no. 6, pp. 1246–1259, 2006.

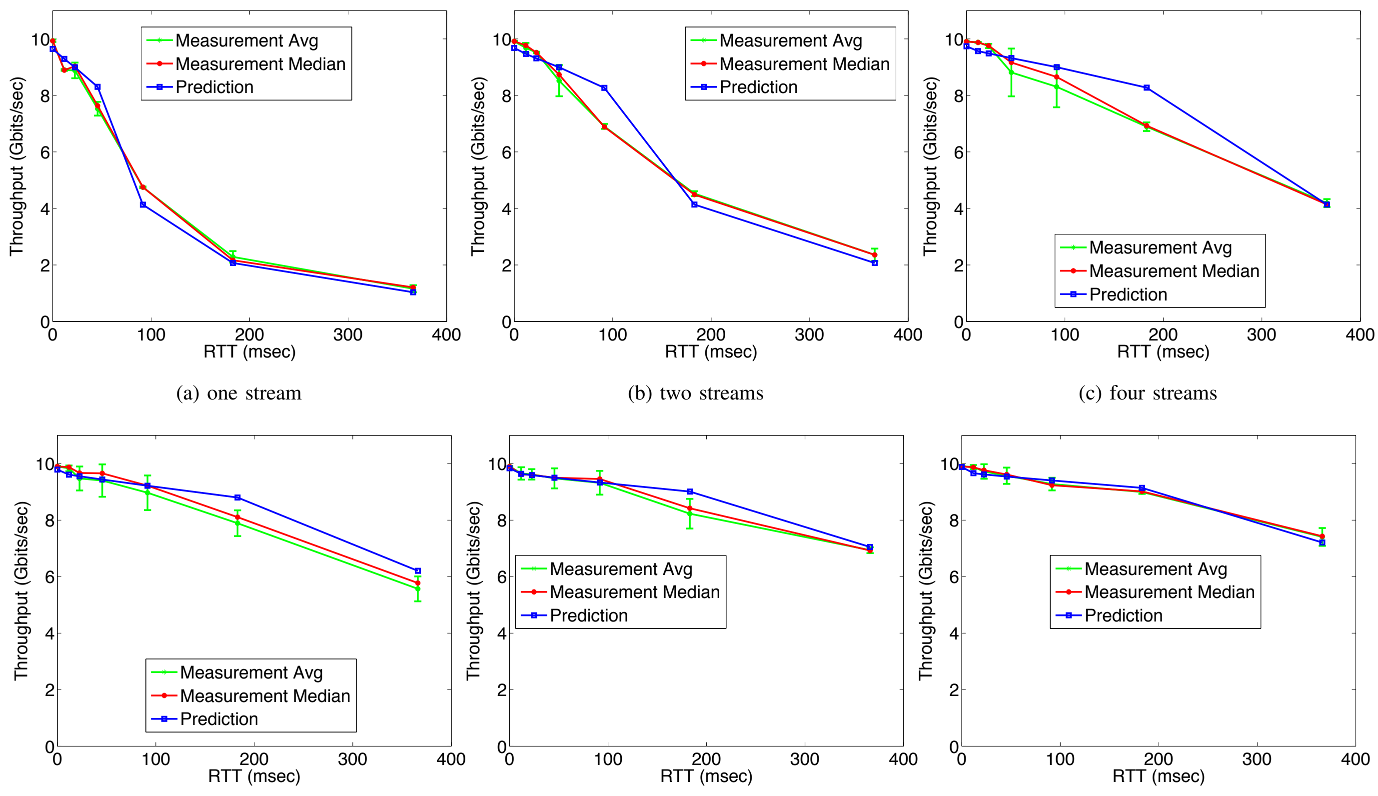

(a) one stream (b) two streams (c) four streams

(d) six streams (e) eight streams (f) ten streams

Fig. 8: Measurement averages and medians vs multiple-stream model predictions for CUBIC.

[3] L. Xu, K. Harfoush, and I. Rhee, "Binary increase congestion control (bic) for fast long-distance networks," in *INFOCOM 2004. Twenty-third AnnualJoint Conference of the IEEE Computer and Communications Societies*, vol. 4, March 2004, pp. 2514–2524 vol.4.

[4] T. Kelly, "Scalable TCP: Improving performance in highspeed wide area networks," *ACM SIGCOMM computer communication Review*, vol. 33, no. 2, pp. 83–91, 2003.

[5] S. Ha, I. Rhee, and L. Xu, "CUBIC: A New TCP-friendly High-speed TCP Variant," *SIGOPS Oper. Syst. Rev.*, vol. 42, no. 5, pp. 64–74, Jul. 2008. [Online]. Available: http://doi.acm.org/10.1145/1400097.1400105

[6] D. Leith and R. Shorten, "H-TCP: TCP for high-speed and long-distance networks," in *Proceedings of PFLDnet*, vol. 2004, 2004.

[7] H. Jamal and K. Sultan, "Performance analysis of TCP congestion control algorithms," *International journal of computers and communications*, vol. 2, no. 1, pp. 18–24, 2008.

[8] Y.-T. Li, D. Leith, and R. N. Shorten, "Experimental evaluation of TCP protocols for high-speed networks," *Networking, IEEE/ACM Transactions on*, vol. 15, no. 5, pp. 1109–1122, 2007.

[9] S. Ha, Y. Kim, L. Le, I. Rhee, and L. Xu, "A step toward realistic evaluation of high-speed tcp protocols," in *Proc. International Workshop on Protocols for Fast Long-Distance Networks (PFLD-net2006)*, 2006.

[10] R. Mbarek, M. T. B. Othman, and S. Nasri, "Performance Evaluation of Competing High-Speed TCP Protocols." *IJCSNS*, vol. 8, no. 6, 2008.

[11] C. Callegari, S. Giordano, M. Pagano, and T. Pepe, "Behavior analysis of TCP Linux variants," *Computer Networks*, vol. 56, no. 1, 2012.

[12] J. Towns, T. Cockerill, M. Dahan, I. Foster, K. Gaither, A. Grimshaw, V. Hazlewood, S. Lathrop, D. Lifka, G. D. Peterson *et al.*, "XSEDE: accelerating scientific discovery," *Computing in Science & Engineering*, vol. 16, no. 5, pp. 62–74, 2014.

[13] W. Allcock, J. Bresnahan, R. Kettimuthu, M. Link, C. Dumitrescu, I. Raicu, and I. Foster, "The Globus Striped GridFTP Framework and Server," in *Proceedings of the 2005 ACM/IEEE Conference on Supercomputing*, ser. SC '05, 2005.

[14] "On-Demand Secure Circuits and Advance Reservation System." [Online]. Available: http://www.es.net/engineering-services/oscars. Accessed May 2016.

[15] S. Ha and I. Rhee, "Taming the elephants: New TCP slow start," *Computer Networks*, vol. 55, no. 9, pp. 2092–2110, 2011.

[16] F. P. Kelly, A. K. Maulloo, and D. K. Tan, "Rate control for communication networks: shadow prices, proportional fairness and stability," *Journal of the Operational Research society*, pp. 237–252, 1998.

[17] R. Srikant, *The mathematics of Internet congestion control*. Springer Science & Business Media, 2012.

[18] V. Misra, W.-B. Gong, and D. Towsley, "Stochastic differential equation modeling and analysis of TCP-windowsize behavior," in *Proceedings of PERFORMANCE*, vol. 99. Citeseer, 1999.

[19] R. El Khoury, E. Altman, and R. El Azouzi, "Analysis of scalable TCP congestion control algorithm," *Computer Communications*, vol. 33, pp. S41–S49, 2010.

[20] W. Bao, V. Wong, and V. Leung, "A Model for Steady State Throughput of TCP CUBIC," in *Global Telecommunications Conference (GLOBECOM 2010), 2010 IEEE*, Dec 2010, pp. 1–6.

[21] D. Leith, R. Shorten, and Y. Lee, "H-TCP: A framework for congestion control in high-speed and long-distance networks," in *PFLDnet Workshop*, 2005.

[22] R. Morris, "TCP behavior with many flows," in *Proceedings of International Conference on Network Protocols*. IEEE, 1997.

[23] S.-y. Yu, N. Brownlee, and A. Mahanti, "Comparative Analysis of Big Data Transfer Protocols in an International High-Speed Network."

[24] M. Bateman, S. Bhatti, G. Bigwood, D. Rehunathan, C. Allison, T. Henderson, and D. Miras, "A comparison of TCP behaviour at high speeds using ns-2 and Linux," in *Proceedings of the 11th communications and networking simulation symposium*. ACM, 2008, pp. 30–37.

[25] J. Crowcroft and P. Oechslin, "Differentiated end-to-end Internet services using a weighted proportional fair sharing TCP," *ACM SIGCOMM Computer Communication Review*, vol. 28, no. 3, pp. 53–69, 1998.